Critical behavior of the three-dimensional compressible Ising antiferromagnet at constant volume: A Monte Carlo study

Luigi Cannavacciuolo and D. P. Landau

Center for Simulational Physics, The University of Georgia, Athens, Georgia 30602, USA

Extensive Monte Carlo simulations in the semi-grand-canonical ensemble are used to study the critical behavior of a three-dimensional compressible Ising model with antiferromagnetic interactions under constant volume conditions. Elastic forces between spins are introduced by the Stillinger-Weber potential and energy parameters are chosen in such a way that antiparallel spin ordering is favored, analogous to the antiferromagnetic coupling in the rigid Ising Hamiltonian. All the quantities analyzed strongly indicate that the system remains in the universality class of the standard (rigid) three-dimensional Ising model, in contrast with theoretical predictions.

I. INTRODUCTION

The Ising model, proposed by Lenz in 1925 as a microscopical model for ferromagnetism, has a (constant) interaction J included only between the nearest-neighbors spins on a (rigid) lattice. Despite its (formal) simplicity an analytical solution has been found only for one- and two-dimensional models in zero magnetic field.[1] For the three-dimensional Ising model only approximate solutions are available [e.g., series expansions,[2] renormalization-group calculations,[3] ϵ expansions,[4] Monte Carlo renormalization-group calculations,[5] and Monte Carlo (MC) simulations[6,7]], although quite precise results have been found.

It was clear, a few years after its introduction, that the Ising model could be employed to describe other phase transitions. For instance, phase separation in binary alloys can be studied by an Ising model in which "up" and "down" spins are replaced with sites occupied by an "*A*"- or "*B*"-type atom, respectively. The chemical potential plays the role of the magnetic field, the density of the magnetization, etc., and the appropriate statistical ensemble is the semi-grand-canonical,[8] instead of the canonical. With the above-mentioned analogy in mind, in the present work we will use the languages of magnetism and alloys interchangeably.

In a real magnetic crystal, however, atoms interact with each other through a combination of elastic and magnetic forces. The next step in realism is, therefore, the explicit introduction of elastic degrees of freedom in the traditionally rigid system. The resulting model is termed *compressible Ising* (CIM). Several empirical potentials have been proposed and employed to mimic the elastic force, from the simple Lennard-Jones to the more specific Tersoff,[9] Keating,[10] Stillinger-Weber,[11] and others (these last three have been introduced, mainly to reproduce the interaction between silicon and germanium atoms in the study of $Si_{1-x}Ge_x$, viewed as Ising binary alloy models).

The issue of how the presence of elastic interactions affects the critical behavior of the Ising model has been intensively studied. In 1954, using thermodynamic considerations,

Rice[12] predicted that if an Ising system with divergent specific heat is put on a deformable lattice at constant pressure, it undergoes a first-order transition. A number of calculations appeared later,[13–15] all of which led to the conclusion that a first-order transition was expected to occur. All these studies assume that a "pure" Ising singularity happens at constant volume. In 1968, Fisher[16] changed the situation drastically with his "hidden variable" theory, assuming that the "pure" phase transition occurs at fixed *intensive* variable, i.e., at fixed pressure. As a result of this hypothesis a second-order transition was found with Fisher-renormalized exponents, if the critical exponent of the specific heat α is positive. A significant highlight in this controversy was the work of Larkin and Pikin,[17] who considered a Hamiltonian with fluctuations of both the order parameter and the elastic modes, and pointed out the special role of the macroscopic mode $\mathbf{k}=0$ (in Fourier space). As a result a first-order transition is found at constant pressure and quadratic coupling of the order parameter and the strain tensor, also if $\alpha=0$. It was later recognized that this result is only valid at low pressure, whereas at high pressure the critical behavior seems to be much more complex.[18,19] A different approach was used by Baker and Essam,[20] who mapped an Ising model onto a compressible lattice, including the coupling between magnetic and elastic degrees of freedom, onto a standard Ising (on a rigid lattice), but with parameters which depend on the elastic degrees of freedom. Both at constant volume and constant pressure, the model exhibited identical critical behavior as the underlying rigid system, but with Fisher-renormalized exponents. This model, as well as others of the same type, however, considers a negligible shear modulus. This somewhat unphysical assumption was soon recognized to be the reason of the disappearance of the first-order transition. Further work[21–24] with more elaborate schemes did not change the result: a first-order transition was always predicted at constant pressure, and a second-order transition with Fisher-renormalized exponents at constant volume. Finally, we cite the long and complicated work by Bergman and Halperin,[25] in which a cubic anisotropy in the elastic forces was introduced. In the isotro-

pic case the same, already established result was obtained, i.e., a first-order transition at constant pressure if $\alpha > 0$, and a second-order transition with renormalized exponents at constant volume. However, this last condition is realized only if the atoms at the surface are fixed, otherwise the system has still enough degrees of freedom to develop a macroscopic instability. In the anisotropic case, however, a so-called microscopic instability was found at constant volume, and this is interpreted as a first-order transition. In his habilitation thesis Dünweg[26] pointed out that the elementary approach taken by Larkin and Pikin is essentially sufficient to understand most of the theoretical results. Starting from the Landau-Ginzburg-Wilson Hamiltonian he was able to show that the CIM under constant pressure exhibits mean-field critical behavior,[27] in agreement with simulations.[28,29] At constant volume he predicted two first-order lines ending in critical points, which are likely to belong to the mean-field universality class. If the magnetic interactions are *antiferromagnetic* (AFM) instead of ferromagnetic,[30] a quadratic coupling between the order parameter and the elastic deformation should be expected. In this case the predictions are: (i) a second-order phase transition with Fisher-renormalized exponents in the case of constant volume[31] (this is in agreement with the ϵ-expansion work of Bergman and Halperin[25]); (ii) a first-order phase transition in the case of antiferromagnetic interactions and constant (zero) pressure.[32] As pressure increases, the first-order line in pressure-temperature space should split into two first-order lines at a triple point. The theoretical prediction in the case of FM interactions at constant volume has been checked by Tavazza *et al.*[33] by MC simulations. In disagreement with theory, they found a closed first-order line which separates ordered and disordered phases.

This result raises the intriguing question of whether or not theory will be correct for the case of AFM interactions and constant volume. This will be the topic of the study that we report here.

II. MODEL AND SIMULATION TECHNIQUES

We use the same model as considered previously in Refs. 29 and 33. We consider a binary alloy of A and B atoms on the nodes of a distortable diamond lattice, free to move on condition that the diamond fourfold coordination is preserved, and that the atomic species on each node may change. The coordination requirement speeds up considerably the simulations as the list of the nearest neighbors of a given atom, which enter the Hamiltonian (see below), is known from the very beginning and does not change during the simulations. The diamond network is decomposed into eight interpenetrating simple cubic sublattices of linear size L, so there are $N = 8L^3$ atoms (sites). Each atom in the system has four degrees of freedom: the three spatial coordinates $\mathbf{r}$ and its species S, which is defined to be $S = 1$ if the atom is an A, or $S = -1$ if it is a B type. The total number of atoms N is kept constant during the simulation, while the relative concentration of A and B particles can vary and is controlled by the chemical potential. The corresponding appropriate statistical ensemble is termed semi-grand-canonical. The Hamiltonian is given by

$$H = -\frac{1}{2}(\mu_A - \mu_B)\sum_i S_i + H_{SW}, \tag{1}$$

where μ_A, μ_B are the chemical potentials of A and B, respectively, and H_{SW} is the Stillinger-Weber (SW) potential given by

$$H_{SW} = H_{2bd} + H_{3bd}. \tag{2}$$

The SW potential contains a two-body interaction H_{2bd} involving nearest neighbors and a three-body interaction H_{3bd} that includes next-nearest neighbors as well. This last term is essential to stabilizing a diamondlike structure. The two-body interaction is given by

$$H_{2bd} = \sum_{\langle i,j \rangle} \epsilon(S_i, S_j)F_2[r_{ij}/\sigma(S_i, S_j)], \tag{3}$$

where

$$F_2(y) = \begin{cases} C_1\left[\dfrac{C_2}{y^p} - 1\right]e^{(b-y)} & \text{if } y < b \\ 0 \text{ otherwise}, \end{cases} \tag{4}$$

where C_1, C_2, p, b are positive constants (for the values see Ref. 29), $\sigma(S_i, S_j) = 2^{1/6}R_0$, R_0 being the ideal distance of the atoms, r_{ij} is the distance between sites i and j, and ϵ is the covalent binding energy. For a binary alloy of silicon and germanium (Si=A, Ge=B) it has been estimated $\epsilon(1,1) = 2.17$ eV, $\epsilon(-1,-1) = 1.93$ eV, and $\epsilon(1,-1) = 2.0427$ eV,[29] and these values were used for elastic ferromagnet simulations.[29,33] In the present work we increased the value for the A-B binding energy by 0.3 eV to favor alternate ordering of A-B particles analogous to the antiferromagnetic ordering in magnets, specifically $\epsilon(1,-1) = 2.3427$ eV. The behavior for this value is expected to be typical of that in the AF regime, but a much larger value could conceivably produce unanticipated effects. A systematic study of the dependence upon the value of $\epsilon(1,-1)$ is beyond the scope of this paper. The three-body part of the Hamiltonian is given by

$$H_{3bd} = \sum_{\langle i,j,k \rangle}\left\{\epsilon(S_i, S_j)^{1/2}\epsilon(S_j, S_k)^{1/2}\mathcal{L}(S_i, S_j, S_k)F_3[r_{ij}/R_0(S_i, S_j), r_{jk}/R_0(S_j, S_k)]\left(\cos\theta_{ijk} + \frac{1}{3}\right)^2\right\}, \tag{5}$$

where $\cos\theta_{ijk} = \mathbf{r}_{ij}\cdot\mathbf{r}_{jk}/|\mathbf{r}_{ij}||\mathbf{r}_{jk}|$;

$$F_3(y_1,y_2) = \begin{cases} e^{[1.2/(y_1-b)+1.2/(y_2-b)]} & \text{if } y_1 < b, \text{ and } y_2 < b \\ 0 & \text{otherwise;} \end{cases} \tag{6}$$

$\mathcal{L} = [\lambda(S_i)\lambda(S_j)\lambda(S_k)]^{1/4}$, with $\lambda(+1) = 21.0$ and $\lambda(-1) = 31.0$ (see Ref. 29). The sum in Eq. (5) is performed over all triplets (i,j,k) with the vertex at site j, i and k are nearest neighbors of j. Note that H_{3bd} contains an angular term which is a sort of angular stiffness essential to stabilizing the diamond lattice (in fact, assigning the bond's length alone is not sufficient, because the lattice has $3N$ translational degrees of freedom, and the bond length only imposes $2N$ constraints). A single MC step (MCS) is performed in the following manner: an atom of species S_i at position $\mathbf{r}_i$ is randomly chosen and a transition to the state $\mathbf{r}_i'$, S_i' is attempted. The change in energy is then calculated and the move is accepted or rejected according to the standard Metropolis criterion. Note that not necessarily both $\mathbf{r}_i'$ and S_i' have to be different from the initial values $\mathbf{r}_i$, S_i. We simulated systems of sizes $L = 4$ ($N=512$), 6 ($N=1728$), 8 ($N=4096$), 10 ($N=8000$), 12 ($N=13\,824$), 14 ($N=21\,952$), and 18 ($N=46\,656$). Periodic boundary conditions were used. A number ranging from 5×10^4 MCS for the smallest systems to 5×10^5 MCS were discarded to thermalize the system. The typical number of MC steps for sampling ranges from 2×10^6 to 6×10^6. For each system size we performed 10-50 independent runs, using different random number sequences to achieve a satisfactory statistical error on the averages of the sampled quantities. During a simulation the volume is kept constant at a value corresponding to the lattice constant a_0 of the ferromagnet, for consistency to the simulations of Refs. 29 and 33. Simulations were performed at a fixed chemical potential $\mu_B = \mu_0$ varying the temperature T, as well as at fixed $T = T_0$ varying μ_B (see Sec. III). In this study we deal with antiferromagnetic ordering and consider atoms sitting on an "even" site to belong to a sublattice SL_1 and those sitting on an "odd" site to belong to a different sublattice SL_2. During the simulations we sampled the SW energy, and the fraction of A and B particles in SL_1 and SL_2. Using these quantities as input, we calculated all the thermodynamic quantities needed by employing the histogram reweighting method.[34]

The order parameter M is defined by the absolute value of the staggered magnetization m^+, i.e.,

$$m^+ = \frac{1}{2N}\left(\sum_{SL_1} S_i - \sum_{SL_2} S_i\right), \tag{7}$$

and

$$M = \langle|m^+|\rangle, \tag{8}$$

where the first and second sums in Eq. (7) are performed over spins belonging to the SL_1 and SL_2 sublattices, respectively. The finite lattice staggered susceptibility of the order parameter is

$$\chi_{fl}^+ = N(\langle m^{+2}\rangle - \langle|m^+|\rangle^2)/k_B T, \tag{9}$$

where k_B is the Boltzmann constant and T the absolute temperature; the staggered susceptibility is

$$\chi^+ = N(\langle(m^+)^2\rangle - \langle m^+\rangle^2)/k_B T. \tag{10}$$

We also determined the average concentration of the B species

$$c_B = \frac{1}{N}\langle n_B\rangle, \tag{11}$$

where n_B is the number of B particles in the system; the reduced fourth-order cumulant of the order parameter

$$U_4 = 1 - \frac{\langle m^{+4}\rangle}{3\langle m^{+2}\rangle^2}; \tag{12}$$

the specific heat

$$C_v = K^2(\langle E^2\rangle - \langle E\rangle^2)/N, \tag{13}$$

where E is the total energy, and $K = 1/k_B T$. In our analysis we considered, in addition, the logarithmic derivatives of m^+ and of U_4 with respect to T. To calculate them we used the relation

$$\frac{\partial}{\partial K}\ln\langle|m^+|^n\rangle = \frac{\langle|m^+|^n E\rangle}{\langle|m^+|^n\rangle} - \langle E\rangle, \quad n = 1,2,\ldots. \tag{14}$$

Moreover, the derivatives of a thermodynamic quantity X with respect to T were calculated using its cross correlation with the energy, i.e.,

$$\frac{\partial\langle|X|\rangle}{\partial K} = \langle|X|E\rangle - \langle|X|\rangle\langle E\rangle. \tag{15}$$

III. MONTE CARLO RESULTS

A. Phase diagram

We started the present study with a rough determination of the phase diagram in the (μ_B, T) plane. We performed simulations at different values of T ranging from 0.05 to 0.35 eV.[35] At fixed T we swept the chemical potential μ_B from 0 to 4 eV at intervals of 0.1 eV, while μ_A was kept constant at 1 eV. For each value of T we determined the value of μ_B at which the maximum value of χ occurs [see Fig. 1(a)]. The behavior of concentration c_B as the chemical potential is swept, is shown in Fig. 1(b). The solid dots indicate the locations of the peaks in the finite lattice ordering susceptibility. The resulting phase boundary is plotted in Fig. 2(a), whereas Fig. 2(b) shows the phase diagram in the (c_B, T) plane. Note that this procedure gives only an approximate phase diagram, which does not take into account extrapolation to the thermodynamic limit. It is, however, very useful as it provides us with information on where to focus in the (μ_B, T) plane with higher-resolution simulations and with finite-size scaling analysis. A transition point from the disordered to the ordered phase is estimated at $\mu_B \simeq 1.42$ eV and $T \simeq 0.34$ eV. We decided, therefore, to keep μ_B fixed at the

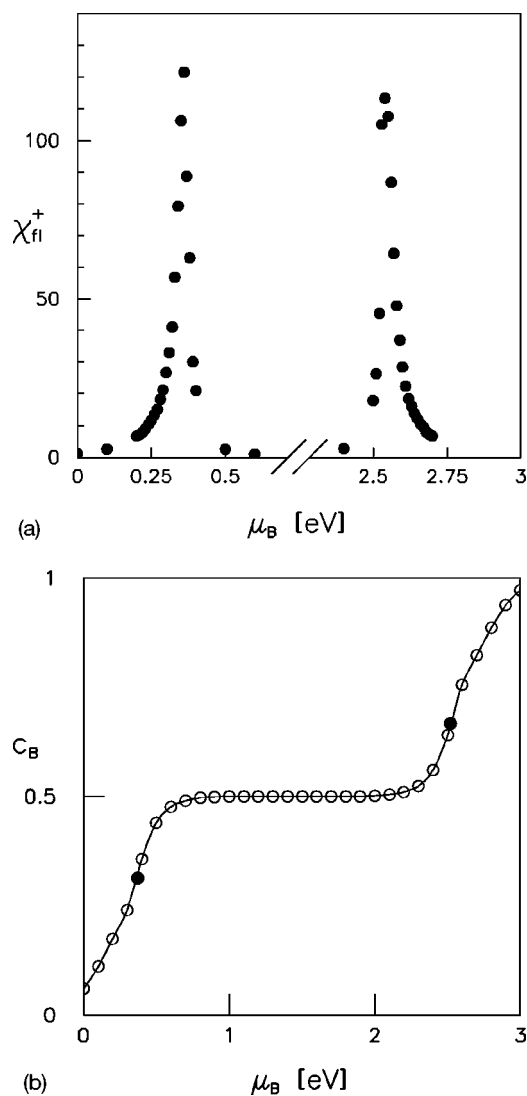FIG. 1. Typical data used to determine the critical points. (a) Plot of χ_{fl}^+ vs μ_B. (b) Concentration of the B species vs μ_B. The bold circles show the location of the transitions. $L=4$ and the temperature is $T=0.1$ eV in both plots. The error bars are smaller than the size of symbols.

above value and to run simulations in a neighbor of $T \simeq 0.34$ eV. This corresponds to moving along the y axis, i.e., perpendicularly to the phase boundary of Fig. 2(a). We also performed simulations at constant $T=0.1$ eV, varying μ_B. The results, not shown in this paper, are consistent with those obtained by moving in the orthogonal direction. Note the slight asymmetry of the curves in Fig. 2, which is a consequence of the three-body interactions. The phase boundary shows no hysteresis, and a finite-size scaling analysis (described in the next section) indicates that the transition is second order.

B. Critical behavior

The critical exponent ν can be determined independently of any other critical quantity, and therefore more accurately. It can be shown that the slope of the cumulant U_4 at the
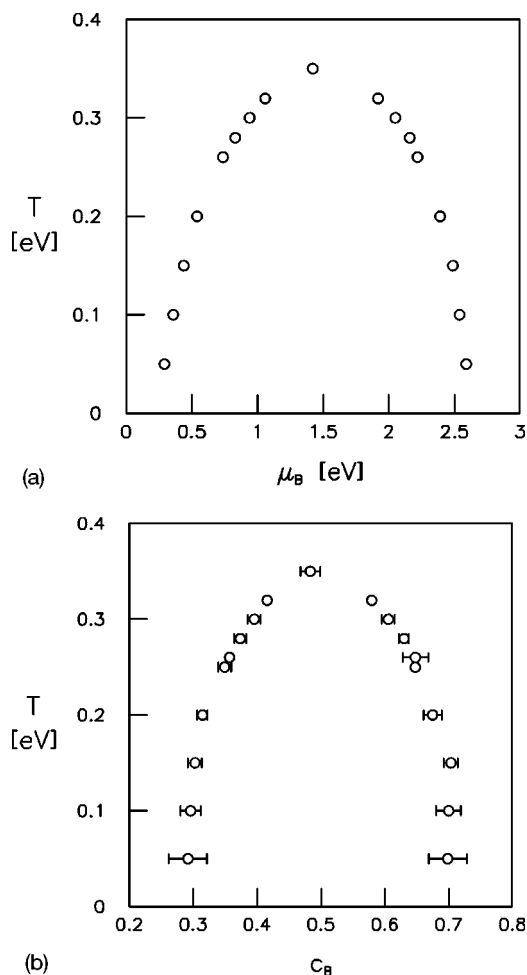

FIG. 2. Phase diagram of the AF compressible Ising model at constant volume in the (μ_B, T) plane (a), and in the (c_B, T) plane (b). The second-order line separates the ordered-disordered phases. Estimates are for $L=4$. Note the slight asymmetry of the curve which reflects the asymmetry of our model. The error bars, if not visible, are smaller than the size of symbols.

critical temperature T_c, or at any other point in the critical region, apart from higher-order corrections, scales with system size as $L^{1/\nu}$.[36] The same scaling behavior is exhibited by the logarithmic derivative of any power of the staggered magnetization. We calculated the derivative of U_4, of $\ln M$ and of $\ln\langle m^{+2}\rangle$ with respect to T, using Eq. (14). Figure 3 displays a log-log plot of the maximum of these derivatives versus L. As expected, they show a linear behavior and they are to a very good approximation parallel. No indication of corrections to scaling is evident. The slopes found after a linear fit to the data are 1.579 ± 0.056, 1.619 ± 0.031, 1.617 ± 0.028, respectively. The average of these values, weighted with the respective errors, gives $\nu=0.620\pm0.008$, which, within the error bars, is in reasonable agreement with the Ising value 0.6295 ± 0.0009 found by MC simulations,[6,7] but is quite different from the theoretically expected Fisher renormalized $\nu'=\nu/(1-\alpha)\simeq0.702$.

Various thermodynamic quantities exhibit an extreme at a certain temperature $T_c(L)$, which depends strongly on that
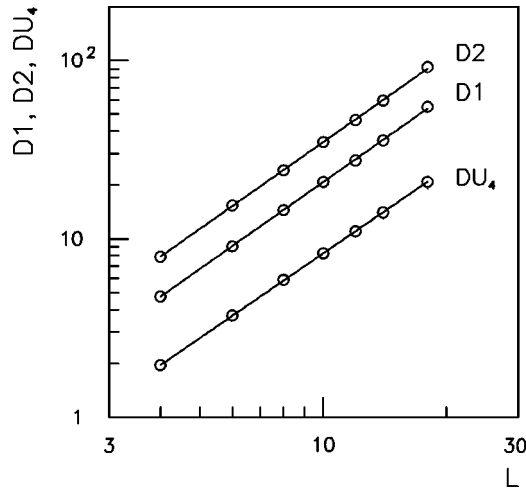
FIG. 3. Determination of the critical exponent ν from the size dependence of the extrema of thermodynamic response functions. From top to bottom: $-\partial \ln\langle m^{+2}\rangle/\partial K$ ($D2$), $-\partial \ln M/\partial K$ ($D1$), $\partial U_4/\partial K$ (DU_4). The error bars are smaller than the size of symbols.

quantity and on the system size. In the asymptotic regime of large systems the following scaling law holds:

$$T_c(L) \sim T_c + A_x L^{-1/\nu}, \tag{16}$$

where the subscript x indicates that the prefactor A depends on the quantity considered. Once ν is determined, Eq. (16) enables us to extrapolate $T_c(L)$ to the thermodynamic limit $L\to\infty$. In Fig. 4 we have plotted $T_c(L)$ of the various quantities examined against $L^{-1/\nu}$, with $\nu=0.620$. The data follow very closely the linear behavior expected, except the two smaller lattice sizes $L=4,6$ for which corrections to scaling are required. We have therefore excluded those data from the
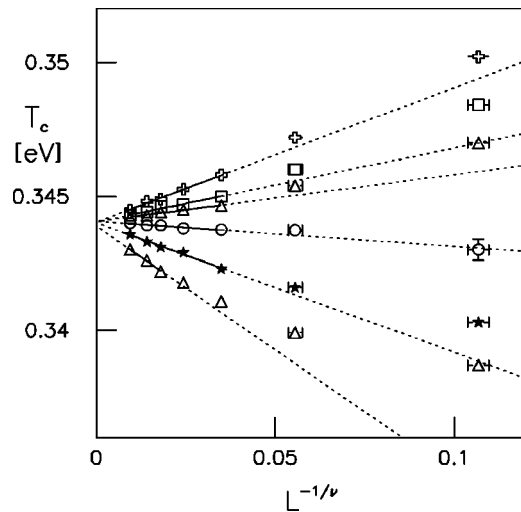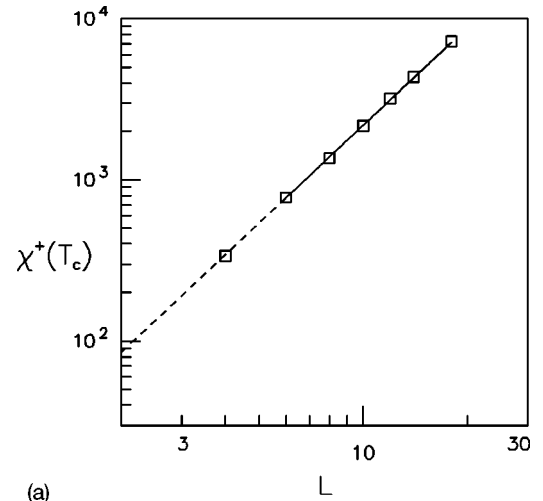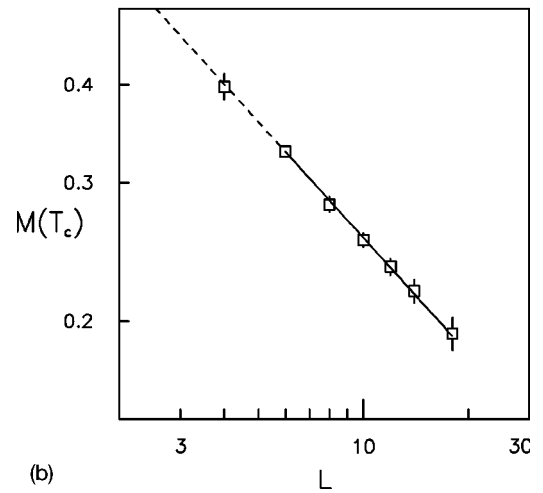

FIG. 4. Extrapolations of the finite system "critical temperature" to the thermodynamic limit for $\mu_B=1.42$ eV. From top to bottom the extreme of: $\partial U_4/\partial K$, $-\partial \ln\langle m^{+2}\rangle/\partial K$, $\partial \ln M/\partial K$, χ, $-\partial M/\partial K$, and C_v. Full lines are fits of Eqs. (16) to the corresponding data. Dotted lines are just extensions of the full ones. The error bars, if not visible, are smaller than the size of symbols.

FIG. 5. Determination of the critical exponents by finite scaling relations. (a) Linear fit of $\chi^+(T_c)$ [Eq. (17)], which provides γ/ν. (b) Linear fit of $M(T_c)$ [Eq. (18)], which provides β/ν. Full lines are fits, dotted lines are just extensions of the full ones. The error bars, if not visible, are smaller than the size of symbols.

extrapolations. The full lines in Fig. 4 are linear fits that account for both the errors on x and y coordinates. The intercepts on the T axis ($L=\infty$) are very close to each other; however, to account for the slight deviations, we have considered the weighted average of these values. The final estimation is $T_c=0.344\,04\pm0.000\,06$ eV.

The critical exponents γ/ν and β/ν can be directly determined from the finite scaling of χ^+ and M, respectively, at T_c. In the asymptotic regime these quantities scale as

$$\chi^+(L,T_c) \sim L^{\gamma/\nu}, \tag{17}$$

$$M(L,T_c) \sim L^{-\beta/\nu}. \tag{18}$$

Figure 5 shows log-log plots of the data. If, again, we exclude the lowest lattice size, the data are found to follow a straight line very well. From a linear fit to the susceptibility we get $\gamma/\nu=2.017\pm0.041$. Using the value previously found for ν, we get $\gamma=1.25\pm0.04$, which, within the errors, is in agreement with the Ising value $\gamma_{\text{Ising}}=1.2390\pm0.0071$ deter-
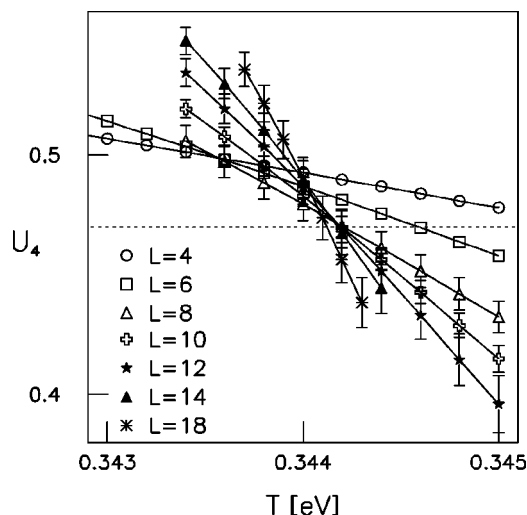
FIG. 6. Plot of the fourth-order cumulant U_4 vs T for different system sizes L. The horizontal dotted line indicates the crossing-point value of the rigid Ising model. The full lines are just a guide for the eyes. The error bars, if not visible, are smaller than the size of symbols.

mined by ϵ expansion,[4] and 1.237 ± 0.002 by MC simulations.[6,7] Analogously, we find $\beta/\nu = 0.491 \pm 0.057$, or $\beta = 0.305 \pm 0.039$, which, within the errors, agrees with the Ising value $\beta_{\text{Ising}} = 0.3270 \pm 0.0015$ (Ref. 4) as well. Note that the error bars on χ^+ and M include both the statistical error on these quantities and the uncertainty in T_c. In fact, this latter turns out to be the major contribution to the overall error bars. We have also tried to determine the critical exponent of the specific heat α. This is however, more difficult to measure because of the presence of an additional fitting parameter. The specific heat is, indeed, expected to scale at T_c as

$$C_v \sim B_1 + B_2 L^{\alpha/\nu}. \qquad (19)$$

The fit of B_1, B_2, and α/ν, not shown here, gives $\alpha/\nu = 0.28 \pm 0.09$, or $\alpha = 0.17 \pm 0.06$, which is in reasonable agreement with the Ising value $\alpha_{\text{Ising}} = 0.110 \pm 0.002$.[7,37] Note that the above procedure provided us with the determination of the critical exponents γ, β, and α not directly, but only via the ratios γ/ν, β/ν, and α/ν. These ratios are the same for Fisher-renormalized exponents.

The fourth-order cumulant U_4 is an important quantity to determine the kind of a phase transition and also to provide an independent determination of the critical temperature. The curves $U_{4,L}(T)$ plotted for different L versus T for large L all cross at T_c.[36] Moreover, the value $U_4(T_c)$ strongly depends on the kind of transition. It has been found that $U_4 \simeq 0.270\,52$ for the mean-field universality class,[38] $U_4 \simeq 0.47$ for the three-dimensional Ising model,[6] and $U_4 \simeq 0.5$ for a first-order transition.[39] If the asymptotic regime has not yet entered, however, curves with different L will cross at different points. Nevertheless, it is still possible to extrapolate the crossing point to $L \rightarrow \infty$. The procedure is described in Ref. 6. Figure 6 displays the behavior of U_4 for our system. For $L \gtrsim 8$ the different curves cross with very good approxima-
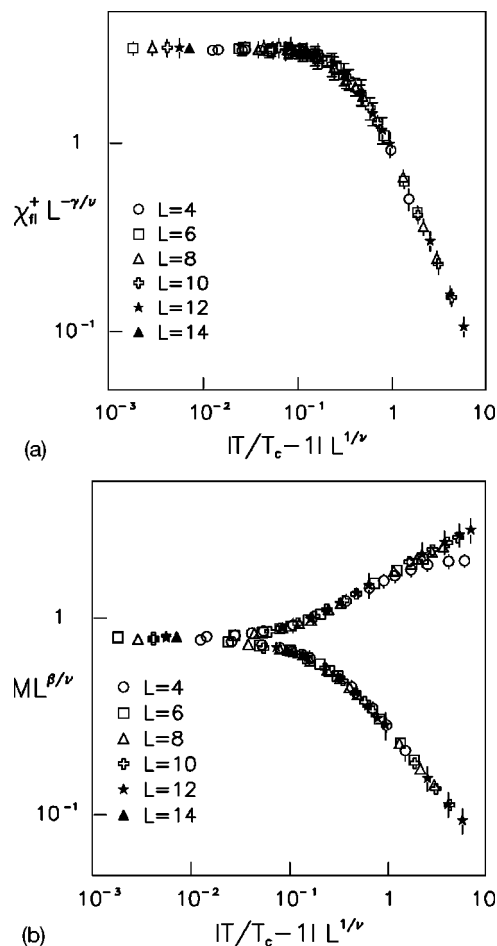

FIG. 7. Data collapsing of the rescaled susceptibility χ^+_{fl} (a), and of the order parameter M (b) vs rescaled temperature $t = |T - T_c|/T_c$, with $T_c = 0.344\,04$ eV. The error bars, if not visible, are smaller than the size of symbols. Data refer to above and below T_c.

tion at the Ising value. The value obtained for the critical temperature using this method is 0.3441 ± 0.0001, which is consistent with the value previously determined.

For a d-dimensional system for which the hyperscaling relation $d\nu = 2 - \alpha$ is valid, the following finite-size laws hold in the vicinity of the critical point

$$\chi^+_{fl}(L,T) = L^{\gamma/\nu} f(t L^{1/\nu}), \qquad (20)$$

$$M(L,T) = L^{-\beta/\nu} g(t L^{1/\nu}), \qquad (21)$$

where $t = 1 - T/T_c$. In a scaling plot of $\chi^+_{fl} L^{-\gamma/\nu}$ (resp. $ML^{\beta/\nu}$) versus $|1 - T/T_c| L^{1/\nu}$ one should, therefore, observe a collapsing of the data. This is exactly what we found, as Fig. 7 demonstrates, and is further evidence of the consistency of the critical exponents and T_c previously determined. Note also that since the data plotted are for above and below T_c, the critical amplitudes corresponding to the two branches in Fig. 7 are thus the same, unlike those for the true susceptibility.[40]

IV. CONCLUSIONS

We have performed Monte Carlo simulations of the compressible Ising model (binary alloy) with antiferromagnetic interactions under constant volume conditions, in the semi-grand-canonical ensemble. Elastic forces are included by the Stillinger-Weber potential. The behavior of all critical quantities analyzed strongly indicated the presence of a closed second-order line with the critical exponents of the (rigid) Ising model. This is in contrast with theories as they predict the occurrence of Fisher-renormalized exponents. Disagreement was also found in the simulations of exactly the same model but with ferromagnetic interactions.[33] The reasons for these disagreements are not clear and should be further investigated. Needless to say, however, that our conclusions should be viewed within the context of any numerical work,

keeping in mind the finiteness of the systems used in the simulations. It is, therefore, clear that, on the basis of these data, the occurrence of a (slow) crossover toward Fisher-renormalized exponents cannot be completely ruled out. A deeper investigation of this issue would require simulations on much larger system sizes, which is, basically, unfeasible with the present computer power. It would be, however, very interesting to investigate the critical behavior under stronger coupling conditions.

[1] L. Onsager, Phys. Rev. **65**, 117 (1944).

[2] B. G. Nickel, in *Phase Transitions: Cargese 1980*, edited by M. Levy, J.-C. Le Guillou, and J. Zinn-Justin (Plenum, New York, 1982), p. 291.

[3] K. G. Wilson, Phys. Rev. B **4**, 3174 (1971).

[4] E. Brezin, J.-C. Le Guillou, and J. Zinn-Justin, Phys. Lett. **47A**, 285 (1974); J.-C. Le Guillou and J. Zinn-Justin, Phys. Rev. B **21**, 3976 (1980); J. Phys. (Paris) **48**, 19 (1987).

[5] G. S. Pawley, R. H. Swendsen, D. J. Wallace, and K. G. Wilson, Phys. Rev. B **29**, 4030 (1984); H. W. J. Blöte, J. de Bruin, A. Compagner, J. H. Croockewit, Y. T. J. C. Fonk, J. R. Heringa, A. Hoogland, and A. L. van Willigen, Europhys. Lett. **10**, 105 (1989); H. W. Blöte, A. Compagner, J. H. Croockewit, Y. T. J. C. Fonk, J. R. Heringa, A. Hoogland, T. S. Smit, and A. L. van Willigen, Physica A **161**, 1 (1989).

[6] A. M. Ferrenberg and D. P. Landau, Phys. Rev. B **44**, 5081 (1991), and references therein.

[7] H. W. J. Blöte, E. Luijten, and J. R. Heringa, J. Phys. A **28**, 6289 (1995).

[8] In the so-called semi-grand-canonical ensemble the number of A and B species may vary on condition that the total number of particles is constant.

[9] J. Tersoff, Phys. Rev. Lett. **56**, 632 (1986).

[10] P. N. Keating, Phys. Rev. **145**, 637 (1966).

[11] F. H. Stillinger and T. A. Weber, Phys. Rev. B **31**, 5262 (1985).

[12] O. K. Rice, J. Chem. Phys. **22**, 1535 (1954).

[13] C. Domb, J. Chem. Phys. **25**, 783 (1956).

[14] D. C. Mattis and T. D. Schultz, Phys. Rev. **129**, 175 (1963).

[15] C. W. Garland and R. Renald, J. Chem. Phys. **44**, 1120 (1963).

[16] M. E. Fisher, Phys. Rev. **176**, 257 (1968).

[17] A. I. Larkin and S. A. Pikin, JETP Lett. **29**, 891 (1969).

[18] Y. Imry, Phys. Rev. Lett. **33**, 1304 (1974).

[19] S. V. Belim and V. V. Prudnikov, Phys. Solid State **43**, 1353 (2001).

[20] G. A. Baker and J. W. Essam, Phys. Rev. Lett. **24**, 447 (1969).

[21] A. F. S. Moreira and W. Figueiredo, Phys. Rev. B **46**, 2891 (1992).

[22] J. Sak, Phys. Rev. B **10**, 3957 (1974); J. Bruno and J. Sak, *ibid.* **22**, 3302 (1980); J. Bruno and J. Sak, *ibid.* **22**, 3319 (1980).

[23] F. Wegner, J. Phys. C **7**, 2109 (1974); H. Wagner and H. Horner, Adv. Phys. **23**, 587 (1974).

[24] J. Oitmaa and M. N. Barber, J. Phys. C **8**, 3653 (1975).

[25] D. J. Bergmann and B. I. Halperin, Phys. Rev. B **13**, 2145 (1976).

[26] B. Dünweg, *Computersimulationen zu Phasenübergängen und kritischen Phänomenen*, Habilitationsschrift, Max-Planck-Institut für Polymerforshung, Mainz (2000).

[27] This is, basically, the same result found by R. A. Cowley, Phys. Rev. B **13**, 4877 (1975), for a type-0 transition.

[28] B. Dünweg and D. P. Landau, Phys. Rev. B **48**, 14 182 (1993).

[29] M. Laradji, D. P. Landau, and B. Dünweg, Phys. Rev. B **51**, 4894 (1995).

[30] The following assumptions are made: (i) Only nearest-neighbor AFM interactions. (ii) Isotropic elasticity, i.e., only two elastic constants are present.

[31] This conclusion is valid if $\alpha > 0$, and at strong coupling. If $\alpha < 0$ Ising exponents are predicted.

[32] This conclusion is valid if $\alpha > 0$. If $\alpha < 0$ Ising exponents are predicted.

[33] F. Tavazza, D. P. Landau, and J. Adler, Phys. Rev. B **70**, 184103 (2004).

[34] A. M. Ferrenberg and R. H. Swendsen, Phys. Rev. Lett. **63**, 1195 (1989).

[35] In the present work, unless otherwise specified, the temperature is quoted as $k_B T$. This permits easy comparison with energy scales used in electronic structure.

[36] K. Binder, Z. Phys. B: Condens. Matter **43**, 119 (1981).

[37] S. A. Antonenko and A. I. Sokolov, Phys. Rev. E **51**, 1894 (1995).

[38] E. Brezin and J. Zinn-Justin, Nucl. Phys. B **257**, 867 (1985).

[39] K. Binder, K. Vollmayr, H. P. Deutsch, J. D. Reger, M. Scheucher, and D. P. Landau, Int. J. Mod. Phys. C **3**, 253 (1992).

[40] A. Pelissetto and E. Vicari, Phys. Rep. **368**, 549 (2002).